THE JOURNAL OF PHYSICAL CHEMISTRY B

Article

pubs.acs.org/JPCB

Effect of the Alkyl Chain Length on the Rotational Dynamics of Nonpolar and Dipolar Solutes in a Series of N-Alkyl-N-Methylmorpholinium Ionic Liquids

Dinesh Chandra Khara, Jaini Praveen Kumar, Navendu Mondal, and Anunay Samanta*

School of Chemistry, University of Hyderabad, Hyderabad-500 046, India

Supporting Information

ABSTRACT: Rotational dynamics of two dipolar solutes, 4-aminophthalimide (AP) and 6-propionyl-2-dimethylamino-naphthalene (PRODAN), and a nonpolar solute, anthracene, have been studied in N-alkyl-N-methylmorpholinium (alkyl = ethyl, butyl, hexyl, and octyl) bis(trifluoromethansulfonyl)-imide (Tf_2N) ionic liquids as a function of temperature and excitation wavelength to probe the microheterogeneous nature of these ionic liquids, which are recently reported to be more structured than the imidazolium ionic liquids (Khara and Samanta, *J. Phys. Chem. B* **2012**, *116*, 13430−13438). Analysis of the measured rotational time constants of the solutes in terms of the Stokes−Einstein−Debye (SED) hydrodynamic theory reveals that with increase in the alkyl chain length attached to the cationic component of the ionic liquids, AP shows stick to superstick behavior, PRODAN rotation lies between stick and slip boundary conditions, whereas anthracene exhibits slip to sub slip behavior. The contrasting rotational dynamics of these probe molecules is a reflection of their location in distinct environments of the ionic liquids thus demonstrating the heterogeneity of these ionic liquids. The microheterogeneity of these media, in particular, those with the long alkyl chain, is further evidence from the excitation wavelength dependence study of the rotational diffusion of the dipolar probe molecules.

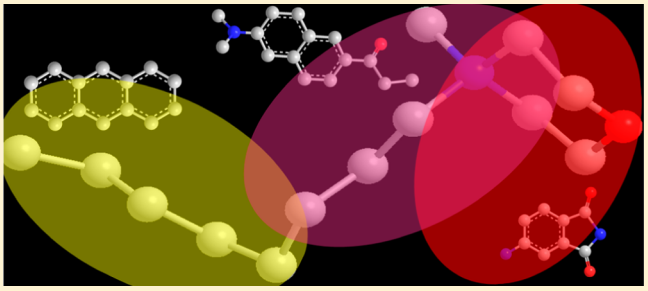

1. INTRODUCTION

The room temperature ionic liquids (RTILs) have now become familiar names among the scientific community for their various applications ranging from reaction media to pharmaceutical drugs and electrolytes in energy storage cell.[1−8] An understanding of the physicochemical properties of the RTILs is essential for better utilization of these substances in different applications.[9−15] The N-alkyl-N-methylmorpholinium ionic liquids, which are found to be more cost-effective compared to the commonly used imidazolium and pyrrolidium salts, have come into prominence, though their physicochemical properties have yet to be explored carefully.[16−20]

As rotational motion of a solute provides useful information on its microenvironment in an unknown medium, the dynamics of rotational diffusion of several fluorescent molecules have been studied by measuring the extent of fluorescence depolarization as a function of time to investigate the structures of various RTILs, which are found to be heterogeneous at the microscopic level,[21−46] and also to study the influence of the various constituents of the RTILs on the rotational dynamics of the probe molecules.[30,47−60] These studies have provided considerable insight into the nature of interaction between the solute and ionic constituents of various RTILs thus shedding light on the microenvironments of these promising, but complex media. We have recently explored a series of N-alkyl-N-methylmorpholinium ionic liquids comprising different alkyl chain lengths by studying the steady-state and time-resolved fluorescence behavior of C153 in these media.[20] A comparison of the fluorescence response of C153 in these and imidazolium ionic liquids seems to suggest that the morpholinium ionic liquids are more structured than the imidazolium ones. Considering that it is possible to obtain considerable insight into the structural organization of the RTILs by studying the rotational dynamics of molecular systems, we probe the organized environments of a series of relatively less explored but promising morpholinium ionic liquids by monitoring the rotational diffusion of two dipolar and one nonpolar probe molecules using time-resolved fluorescence anisotropy measurements.

In this context, we note that there are only a limited number of studies where the effect of the chain length of one of the constituents of the RTILs on the rotational dynamics is studied.[30,49,50,54,56] Maroncelli and co-workers studied the rotational dynamics of C153 in several ammonium ionic liquids comprising different chain lengths of the cation.[56] Other than the expected influence of viscosity of the RTILs no other factor was found to influence the rotational diffusion of the solute. Fruchey and Fayer studied the rotational dynamics of negatively charged (sodium 8-methoxypyrene-1,3,6-sulfonate, MPTS), and neutral (perylene) molecules in a series of N-alkyl-

Received: January 27, 2013
Revised: March 4, 2013
Published: April 1, 2013

dx.doi.org/10.1021/jp400914y | *J. Phys. Chem. B* 2013, 117, 5156−5164

N-methylimidazolium ionic liquids.[30] They observed superstick behavior of the charged molecule, MPTS, due to its strong hydrogen bonding interaction with the imidazolium cation of the RTILs and slip to sub slip behavior of the neutral molecule, perylene. The rotational dynamics of perylene in the octyl chain containing ionic liquid is found to be similar to that in paraffin oil. Dutt also studied the rotational dynamics of a charged probe (R110) and a neutral probe (DMDPP) in different N-alkyl-N-methylimidazolium ionic liquids.[54] While the author found that rotational time constants of R110 shift toward the stick boundary condition with increase in alkyl chain length of the ionic liquids due to specific hydrogen bonding interaction between the solute and RTILs, no influence of the alkyl chain length of cation was observed on the rotational dynamics of DMDPP. Recently, Das and Sarkar have also studied the rotational dynamics of two neutral solutes (AP and C153) in imidazolium ionic liquids comprising anions with different alkyl chain length.[50] They found AP rotation to follow the stick boundary condition due to its specific interaction with the RTILs, whereas C153 rotation changes from slip to sub slip behavior with increase in the alkyl chain length of the anion. The latter was explained on the basis of increase in size of the RTIL with respect to the solute. Very recently, Gangamallaiah and Dutt have studied the rotational dynamics of neutral (9-phenylanthracene, 9-PA) and charged (both cationic, R110, and anionic, fluorescein, FL) molecules in several 1-alkyl-3-methylimidazolium ionic liquids to study the effect of the alkyl chain length on the rotational dynamics of the solute.[49] However, they did not observe any effect of the alkyl chain length on the solute rotation; the neutral probe was found to follow the slip boundary condition and the ionic probes followed close to stick boundary condition according to the SED model.

In this work, we have chosen three specific neutral solutes (two dipolar molecules, namely, AP, PRODAN, and one nonpolar molecule, anthracene; Chart 1) to explore the physicochemical properties of these less explored, but promising morpholinium ionic liquids by studying the rotational dynamics. AP is selected due its ability to enter into specific hydrogen bonding interaction with hydrogen bond donors/acceptors.[50,59] PRODAN and anthracene, which have comparable volume, are chosen due to their preference to different environments of an organized assembly consisting of polar and nonpolar domains.[61,62] While most of the measurements have been performed by exciting the molecules at wavelength corresponding to the peak of the first absorption maximum, the experiments on dipolar probes have also been carried out by exciting them at wavelength, which corresponds to the red-edge of the first absorption band with a view to probing the heterogeneity of the media from another angle.

Chart 1. Chemical Formula and Abbreviations of the RTILs and Probe Molecules

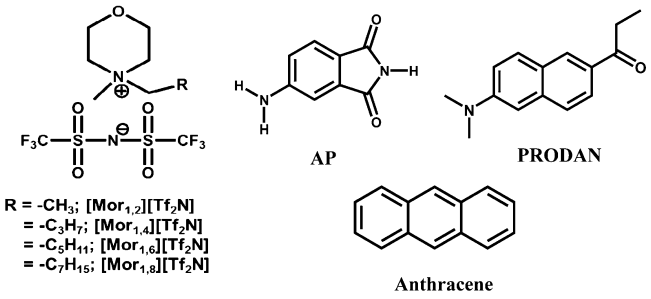

2. EXPERIMENTAL SECTION

2.1. Materials. PRODAN procured from Molecular probes was used as received. AP and anthracene were obtained from TCI and Sigma Aldrich, respectively, and were recrystallized from ethanol prior to use. Alkyl bromides, acetone, acetonitrile, and dichloromethane (DCM) were obtained from Merck (India) and were distilled prior to use. N-Methylmorpholine and bis(trifluoromethanesulfonyl)imide lithium salt ($LiTf_2N$) were procured from Sigma Aldrich and used as received.

2.2. Synthesis of $[Mor_{1,n}][Tf_2N]$. These RTILs were synthesized by following a two-step procedure.[16] The first step involved preparation of the bromide salt of N-alkyl-N-methylmorpholinium ion, $[Mor_{1,n}][Br]$, and the second step consisted of exchange of the bromide ion by the bis-(trifluoromethanesulfonyl)imide ion. The procedure followed for the synthesis of the RTILs is outlined below. The alkyl bromide was slowly added to an acetonitrile solution of N-methylmorpholine and then the solution was refluxed at 80 °C for 6−8 h. Subsequently, acetonitrile was removed from the reaction mixture in a rotary evaporator. The bromide salt, $[Mor_{1,n}][Br]$, was washed with acetone several times to remove the unreacted materials from the reaction mixture. The salt was dried under vacuum and weighed for the next step. In the second step, an aqueous solution of the bromide salt was first treated with activated charcoal under reflux condition for overnight and then the filtrate were used for a metathesis reaction by adding lithium bis(trifluoromethanesulfonyl)imide and stirring for nearly 24 h. Then DCM was added to the solution and the organic layer was separated out from the reaction mixture. Subsequently, the organic layer was washed several times with water until it was found free from any halide (checked with a $AgNO_3$ solution). Finally, DCM was removed from the mixture and the RTIL was dried for several hours under high vacuum prior to use.

2.3. Instrumentation. The viscosities of the ionic liquids were measured by a LVDV-III Ultra Brookfield Cone and Plate viscometer (1% accuracy and 0.2% repeatability). The viscosities at different temperatures were measured by using a water circulator (Julabo). The absorption and steady-state fluorescence spectra were recorded on a UV−visible spectrophotometer (Cary100, Varian) and spectrofluorometer (FluoroLog, Horiba Jobin Yvon), respectively. The fluorescence spectra were corrected for the instrumental response. Time-resolved anisotropy decay measurements were carried out using a time-correlated single-photon counting (TCSPC) spectrometer (Horiba Jobin Yvon IBH). Diode lasers (λ_{exc} = 375 and 439 nm) were used as the excitation source, and an MCP photomultiplier (Hamamatsu R3809U-50) was used as the detector (response time 40 ps). The instrument response function (IRF) of the setup (80 and 100 ps) was limited by the full-width at half-maximum (fwhm) of the exciting laser pulse, respectively. The lamp profile was recorded by placing a scatterer (dilute solution of Ludox in water) in place of the sample. Decay curves were analyzed by nonlinear least-squares iteration procedure using IBH DAS6 (version 2.2) decay analysis software. The quality of the fits was assessed by the χ^2 values and distribution of the residuals. The temperature-dependent studies were performed by using a water circulator (Julabo).

dx.doi.org/10.1021/jp400914y | J. Phys. Chem. B 2013, 117, 5156−5164

Table 1. Rotational Relaxation Times[a] of the Probes in Four Morpholium RTILs as a Function of Temperature and Excitation Wavelength

			rotational relaxation time in ns				
			AP		PRODAN		Anthracene
ILs	temp (K)	viscosity (cP)	λ_{ex} = 375 nm	λ_{ex} = 439 nm	λ_{ex} = 375 nm	λ_{ex} = 439 nm	λ_{ex} = 375 nm
$[Mor_{1,2}][Tf_2N]$	308	147	6.35	7.02	5.62	6.10	1.54
	318	85	3.76	4.25	4.20	4.26	0.90
	328	52	2.33	2.73	2.78	2.88	0.55
	338	34	1.52	1.71	1.94	2.05	0.36
$[Mor_{1,4}][Tf_2N]$	298	503	24.49	28.53	8.77	8.96	4.25
	308	236	12.11	12.80	8.17	8.87	2.27
	318	126	6.44	7.92	5.83	6.27	1.44
	328	72	3.73	4.45	3.81	4.17	0.98
	338	45	2.29	2.41	2.35	2.62	0.74
$[Mor_{1,6}][Tf_2N]$	298	578	32.07	36.30	8.70	9.26	3.31
	308	269	16.50	20.94	7.35	8.05	2.40
	318	142	9.50	10.46	6.21	6.91	1.59
	328	80	5.35	6.00	3.70	4.26	1.11
	338	48	3.26	3.77	2.49	2.84	0.78
$[Mor_{1,8}][Tf_2N]$	298	673	36.0	41.40	14.18	19.90	3.25
	308	327	21.10	21.98	8.56	12.83	2.03
	318	183	12.31	12.50	6.06	9.80	1.36
	328	113	7.03	8.03	3.94	5.74	0.86
	338	76	4.37	4.64	2.84	3.80	0.62

[a] ±10%. The fluorescence lifetimes of AP, PRODAN, and anthracene measured in $[Mor_{1,8}][Tf_2N]$ are around 18.2, 4.3, and 3.5 ns, respectively.

2.4. Method. The anisotropy measurements were performed using two polarizers by placing one of them in the excitation beam path and the other in front of the detector. An alternate collection of the fluorescence intensity in parallel (I_{II}) and perpendicular ($I_{\perp}$) polarization (with respect to the vertically polarized excitation laser beam) for equal interval of time was made until the count difference between the two polarizations (at $t = 0$) was ~5000. For G-factor calculation, the same procedure was followed, but with only 4 cycles and horizontal polarization of the exciting laser beam. The anisotropy measurements were performed at the respective fluorescence maxima of the probe using a monochromator with a bandpass of 2 nm. Time-resolved fluorescence anisotropy, $r(t)$, is calculated using the following equation

$$r(t) = \frac{I_{II}(t) - GI_{\perp}(t)}{I_{II}(t) + 2GI_{\perp}(t)} \quad (1)$$

where G is the correction factor for the detector sensitivity to the polarization direction of the emission, which depends on both the excitation source and the monitoring wavelength. $I_{II}(t)$ and $I_{\perp}(t)$ are the fluorescence decays polarized parallel and perpendicular to the polarization of the excitation light, respectively. The rotational time constants were estimated by fitting the anisotropy decay profiles to a single or biexponential function depending on the situation.

3. RESULTS AND DISCUSSION

The time-resolved fluorescence anisotropy measurements in RTILs have been performed over a temperature range of 25−65 °C except in $[Mor_{1,2}][Tf_2N]$ in which the study is carried out in the temperature range of 35−65 °C. In addition, the measurements on the two dipolar probes AP and PRODAN are carried out using two different excitation wavelengths (375 and 439 nm). The rotational relaxation times are estimated from the single or biexponential fit to the anisotropy decay profiles (depending on the quality of the fit judged by the χ^2 values and plot of residuals). In the latter case, the average value of the two time constants was used as the two rotational times of the probe molecule. It is to be noted that, except in $[Mor_{1,2}][Tf_2N]$, the rotational time constants were obtained from the biexponential to the anisotropy decay profiles.

3.1. AP. The rotational relaxation times of AP in four ionic liquids at various temperatures for two different excitation wavelengths are presented in Table 1. The results show that, at any given temperature, the rotational relaxation time increases with increase in the alkyl chain length of the cation and decreases with increase in temperature. This trend is understandable considering the fact that the viscosity of the RTILs increases with increase in the alkyl chain length of the cation and decreases with increase in temperature.

The rotational times measured by exciting the sample at the red edge of the first absorption band (439 nm) show a similar trend. It is interesting to note, however, the difference in the rotational time constants for two different excitations, which though is negligible in $[Mor_{1,2}][Tf_2N]$, is clearly noticeable in the longest chain length containing RTIL, $[Mor_{1,8}][Tf_2N]$, particularly near the room temperature (Figure 1).

3.2. PRODAN. The measured rotational time constants of PRODAN in four different ionic liquids at various temperatures for two different excitation wavelengths are collected in the Table 1. The effect of temperature and alkyl chain length on the rotational time constants of PRODAN is very similar to that observed for AP, i.e., the rotational time increases with increase in chain length of the alkyl group and decreases with increase in temperature of the medium. However, unlike AP, PRODAN does not show appreciable variation of the rotational time with change of alkyl chain length of the cation.

For PRODAN, excitation at 439 nm also gives a higher rotation time constant compared to 375 nm excitation. While the overall trend of variation of the rotational time with alkyl

dx.doi.org/10.1021/jp400914y | J. Phys. Chem. B 2013, 117, 5156−5164

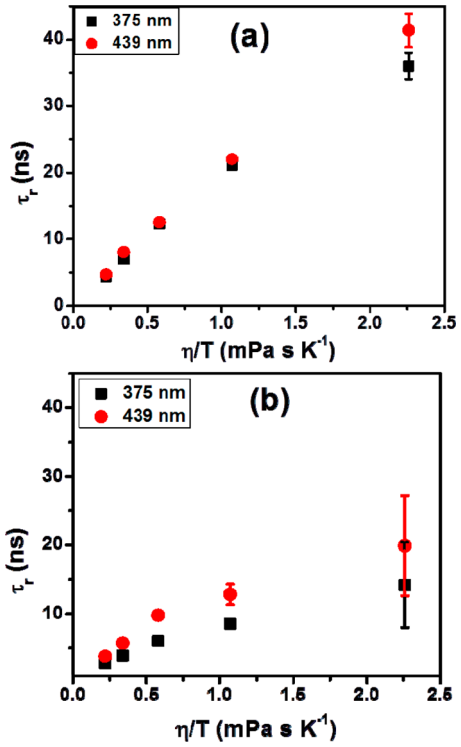

Figure 1. Excitation wavelength dependence of τ_r of AP (a) and PRODAN (b) on η/T in $[Mor_{1,8}][Tf_2N]$.

chain length of the cation and temperature is found similar to that observed for AP, the dependence of the rotational time of PRODAN on excitation wavelength is found more pronounced than in the previous case (Figure 1).

3.3. Anthracene. Rotational dynamics of the nonpolar solute, anthracene, in these RTILs is found to be quite interesting and very different from those of the dipolar probes, AP and PRODAN. Instead of an increase in rotational time constant, a decrease is observed with increase in viscosity of the ionic liquids as the length of the alkyl chain attached to the cation is increased (Table 1). The effect of temperature on the rotational dynamics is, however, found to be similar to that observed for the two dipolar solutes.

In order to understand the rotational dynamics of the solutes we have analyzed our experimental results using the Stokes–Einstein–Debye (SED) hydrodynamic theory, which is the most commonly used model of rotational diffusion. According to this theory, the reorientation time (τ_r) of a noninteracting solute in a solvent continuum of viscosity η is given by

$$\tau_r = \frac{V_h \eta}{k_B T} \qquad (2)$$

where V_h is the hydrodynamic volume of the solute, which is a product of the van der Waals volume (V) of the molecule, its shape factor (f), and boundary condition parameter (C), k_B is the Boltzmann constant, and T is the absolute temperature of the system. The shape factor (f), introduced by Perrin to take into account the nonspherical shape of a solute, is a function of the axial ratio of the semi axes and is greater than 1. For a spherical solute, $f = 1$. The boundary condition parameter, C, is unity when the size of the rotating solute is much bigger than the solvent molecule. This represents the stick boundary condition. However, in the case of solute having a size smaller or comparable to the solvent molecule, C, is given by $0 < C < 1$.

It is to be noted that τ_r, given by eq 2, is a measure of mechanical or hydrodynamic friction experienced by the solute molecule. The axial lengths, van der Waals volumes, and shape factors for the probe molecules used in this study are taken from the literature[57] and the boundary conditions are calculated according to the reported procedure.[48,52] These values are collected in Table 2.

Table 2. Dimension,[a] van der Waals Volume,[a] Shape Factor (f),[a] and Boundary Condition Parameter (C_{slip}) of the Probe Molecules Calculated from the SED Hydrodynamic Theory

probe	axial radii /Å^3	volume /Å^3	f	C_{slip}
AP	5 × 3.5 × 1.8	134	1.6	0.11
PRODAN	7.7 × 3.9 × 1.8	227	2.4	0.19
Anthracene	5.9 × 3.9 × 1.8	175	1.3	0.29

[a]Values are taken from ref 57.

The analysis of the experimental results in terms of the SED hydrodynamic model reveals that AP changes from stick to superstick behavior with increase in alkyl chain length of the RTILs, which is highlighted in Figure 2. The rotational dynamics of AP on excitation at a longer wavelength also follows a similar change from the stick to superstick behavior (Figure S1 of the Supporting Information).

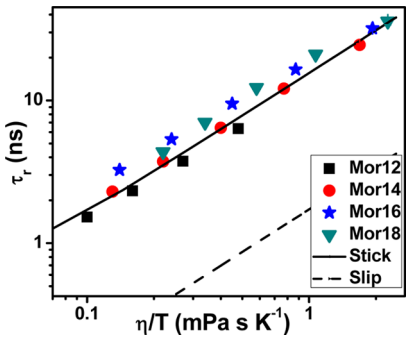

Figure 2. Plot of τ_r of AP versus η/T in different RTILs. The points indicate the experimentally measured rotational times (τ_r^{expt}). The lines represent the stick (solid) and slip (dash) boundary conditions, computed according to the SED hydrodynamic model (λ_{exc} = 375 nm).

Figure 3 shows that the rotational relaxation times of PRODAN lie between the slip and stick boundary conditions. One also observes a gradual shift toward the slip to sub slip boundary condition at low temperature with increase in alkyl chain length of the cation. At higher temperature, however, the rotational time constants vary linearly with η/T irrespective of the alkyl chain length of the cation. The excitation wavelength dependent rotational constants also show a similar behavior (Figure S2 of the Supporting Information).

The rotational time constants of anthracene do not lie between the slip and stick boundary conditions of the SED hydrodynamic model (Figure 4). The rotational relaxation time shifts from slip to sub slip regime with increase in chain length of the alkyl group of the cation. Another interesting point to note is that at higher temperatures the rotational time constants lie on the slip boundary line in all RTILs except in $[Mor_{1,8}][Tf_2N]$, where the values are far apart from the slip boundary line.

dx.doi.org/10.1021/jp400914y | J. Phys. Chem. B 2013, 117, 5156–5164

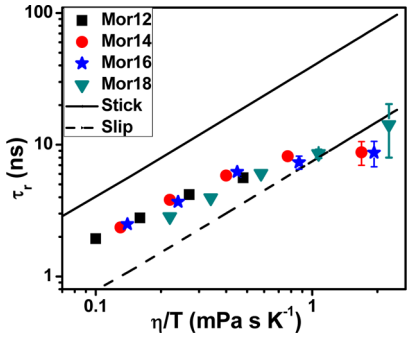

Figure 3. Plot of τ_r of PRODAN versus η/T in different RTILs. The points indicate the experimentally measured rotational times (τ_r^{expt}). The lines represent the stick (solid) and slip (dash) boundary conditions, computed according to the SED hydrodynamic model (λ_{exc} = 375 nm).

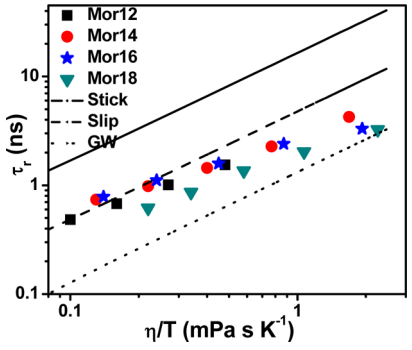

Figure 4. Plot of τ_r of anthracene versus η/T in different RTILs. The points indicate the experimentally measured rotational times (τ_r^{expt}). The computed lines represent the stick (solid) and slip (dash) boundary conditions, according to the SED hydrodynamic model. The third line (dot) represents the quasi-hydrodynamic Gierer-Wirtz model (λ_{exc} = 375 nm).

In the case of a deviation of the rotational relaxation dynamics from the slip boundary condition of the SED model, quasi-hydrodynamic models like Gierer-Wirtz (GW) and Dote-Kivelson-Schwartz (DKS) are used to explain the experimental results.[63−66] In the present case, we attempt to analyze our results in terms of the GW theory,[67] which assumes the solvent to be made of concentric shells of spherical particles surrounding the spherical solute. The boundary condition parameter (C_{GW}) is calculated by considering how the angular velocity of the solvent molecules in successive shells surrounding the solute decreases as a function of the distance away from it. The expression for C_{GW} is given by[49]

$$C_{GW} = \sigma C_0 \tag{3}$$

where, σ, sticking factor, is given by[49]

$$\sigma = \left[1 + 6\left(\frac{V_s}{V_p}\right)^{1/3} C_0\right]^{-1} \tag{4}$$

and C_0 is

$$C_0 = \left\{\frac{6\left(\frac{V_s}{V_p}\right)^{1/3}}{\left[1 + 2\left(\frac{V_s}{V_p}\right)^{1/3}\right]^4} + \frac{1}{\left[1 + 4\left(\frac{V_s}{V_p}\right)^{1/3}\right]^3}\right\}^{-1} \tag{5}$$

In these equations, V_s and V_p are the van der Waals volume of the solvent and solute, respectively. In the present case, a volume of 421 Å^3 (obtained from the Edwards volume increment method[68]) was used as V_s for $[Mor_{1,8}][Tf_2N]$. The computed rotational time constant according to the GW model shows that the experimental rotational time constant of anthracene follows neither slip nor GW boundary condition, but it lies between the two (Figure 4).

The above analysis reveals that the rotational dynamics of three neutral solutes are quite different in any given RTIL. This difference in the rotational relaxation behavior of the solutes can be due to the difference in the nature of interaction between the solute and solvent. However, a detailed analysis of the results, as described below, suggests otherwise.

Both stick and superstick rotational dynamics of AP in conventional solvents and ionic liquids are known, when AP is hydrogen bonded with the solvent molecule.[50,59,69] In the present case, the hydrogen bonding interaction of the N−H proton of AP with the F atom of $[Tf_2N]^-$ and/or the O atom of the morpholinium cation can contribute to the stick and superstick behavior of the rotational diffusion of AP. Figure 5,

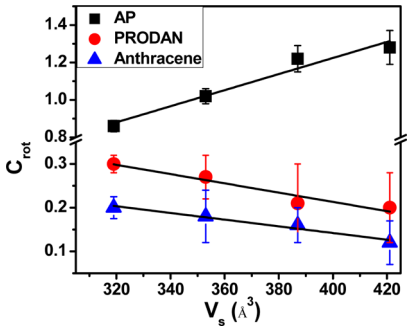

Figure 5. Plot of rotational coupling constant (C_{rot}, 308 K) versus van der Waals volume (V_s) of the RTILs (λ_{exc} = 375 nm). The solid lines represent linear fit to the data points.

which depicts the variation of the coupling constants ($C_{rot} = \tau_r^{expt}/\tau_r^{stick}$) with the van der Waals volumes of the RTILs, shows that the increase (49%) of C_{rot} in the case of AP is not very different from the increase (32%) in van der Waals volume of ionic liquids for a change of the alkyl group from ethyl to octyl, thus supporting strong hydrogen bonding interaction between this probe molecule and the RTILs. In this context, it is to be noted that a recent study in imidazolium ionic liquids shows no regular variation of C_{rot} with increase in the chain length attached to the cation despite specific hydrogen bonding interaction between the solutes and RTILs.[49] Our observation of a steady variation of the coupling constant (near room temperature) with alkyl chain length of the cation is, however, similar to that reported by others.[30,54] The linearity of the τ_r values with η/T in different RTILs that can be judged from the p values by fitting the data to $\tau_r = A(\eta/T)^p$, indicates strong hydrogen bonding between AP and RTILs still persists even at higher temperatures.

dx.doi.org/10.1021/jp400914y | J. Phys. Chem. B 2013, 117, 5156−5164

$$[\mathrm{Mor}_{1,2}][\mathrm{Tf_2N}]: \tau_r = (12.41 \pm 0.05)\left(\frac{\eta}{T}\right)^{0.91\pm0.001}$$

$$(N = 4, R = 1)$$

$$[\mathrm{Mor}_{1,4}][\mathrm{Tf_2N}]: \tau_r = (15.17 \pm 0.07)\left(\frac{\eta}{T}\right)^{0.92\pm0.01}$$

$$(N = 5, R = 0.9998)$$

$$[\mathrm{Mor}_{1,6}][\mathrm{Tf_2N}]: \tau_r = (18.41 \pm 0.11)\left(\frac{\eta}{T}\right)^{0.85\pm0.01}$$

$$(N = 5, R = 0.9998)$$

$$[\mathrm{Mor}_{1,8}][\mathrm{Tf_2N}]: \tau_r = (18.73 \pm 0.61)\left(\frac{\eta}{T}\right)^{0.82\pm0.05}$$

$$(N = 5, R = 0.9944)$$

In the case of PRODAN, even though the time constants lie between the slip and stick boundary conditions, the rotational time constants gradually shift toward the slip and subslip boundary condition at low temperatures with increase in the chain length of the cation. However, at higher temperature, the effect of the alkyl chain length on rotational dynamics is not observable. The plot in Figure 5 shows a steady decrease in the coupling constant with increase in van der Waals volumes of the RTILs. This behavior clearly indicates that the nature of the interaction of PRODAN with the RTILs changes with a change in the alkyl chain length of the cation. This is possible only if there is a phase separation of the RTIL into hydrophilic and hydrophobic domains with increase in alkyl chain length, and the probe molecule relocates itself in the hydrophobic domain.[20] In addition to the decrease of the coupling constants with increase in the alkyl chain length of cation, a deviation from the linearity of the τ_r values with η/T is evident from the degree of nonlinearity (the value of the p parameter) of $\tau_r = A(\eta/\mathrm{T})^p$.

$$[\mathrm{Mor}_{1,2}][\mathrm{Tf_2N}]: \tau_r = (9.2 \pm 0.6)\left(\frac{\eta}{T}\right)^{0.64\pm0.05}$$

$$(N = 4, R = 0.9888)$$

$$[\mathrm{Mor}_{1,4}][\mathrm{Tf_2N}]: \tau_r = (7.58 \pm 0.6)\left(\frac{\eta}{T}\right)^{0.41\pm0.1}$$

$$(N = 5, R = 0.8829)$$

$$[\mathrm{Mor}_{1,6}][\mathrm{Tf_2N}]: \tau_r = (7.13 \pm 0.5)\left(\frac{\eta}{T}\right)^{0.40\pm0.07}$$

$$(N = 5, R = 0.9078)$$

$$[\mathrm{Mor}_{1,8}][\mathrm{Tf_2N}]: \tau_r = (8.26 \pm 0.11)\left(\frac{\eta}{T}\right)^{0.66\pm0.02}$$

$$(N = 5, R = 0.9982)$$

In the present case, the degree of nonlinearity is quite large and the p values lie between 0.40 and 0.66. Generally the fitting parameter p for a large number of molecules studied both in RTILs and conventional solvents is close to unity,[47,48,51−54,63] except in higher n-alkanes where it is around 0.63.[63] The τ_r vs η/T plots and the degree of nonlinearity in long chain containing RTILs are quite similar to the rotational dynamics of a solute in higher n-alkanes.[63] This suggests that PRODAN is mostly surrounded by the alkyl groups of the RTILs. It should be noted in this context that, at temperature around $1.2T_g$, the conventional solvents become heterogeneous when a poor p value ($0.25 \le p \le 0.75$) is observed.[70−73] The poor degree of linearity near room temperature, which is an indication of the departure from the SED hydrodynamic model, is similar to that observed previously for C153 in these RTILs.[20] The only difference is that the degree of nonlinearity is much more prominent for PRODAN compared to C153. Therefore, the present results substantiate the domain structure of these RTILs. PRODAN seems to locate itself mainly at the hydrophobic domain in long chain length containing RTILs. The association of PRODAN with the alkyl moieties creates void space through which the molecule can rotate with little hindrance, leading to a faster rotational relaxation near room temperature. A similar rotational dynamics of PRODAN in RTILs comprising different chain lengths at higher temperatures (Figure 3) indicates that the domain structure of the RTILs is perturbed/lost under this condition.

In the case of anthracene, as the experimental rotational time constants lie between the computed slip line of the SED model and the GW boundary line, the results cannot be explained by either SED or GW model. Moreover, the coupling constants are found to decrease steadily with increase in the van der Waals volumes of the RTILs (Figure 5), near or just above the room temperature, a trend which is similar to that made for PRODAN as well.[74] A steady decrease of the C_{rot} values suggests that the nature of interaction between anthracene and RTILs varies with the alkyl chain length of the cation. This can only be explained considering separation of the medium into hydrophobic and hydrophilic domains with anthracene positioning itself in the hydrophobic domain of the RTILs, where it experiences less friction due to not so tight packing by the alkyl chain of the cation.[20,63] A similar picture emerges when one inspects the p values of $\tau_r = A(\eta/T)^p$.

$$[\mathrm{Mor}_{1,2}][\mathrm{Tf_2N}]: \tau_r = (2.66 \pm 0.02)\left(\frac{\eta}{T}\right)^{0.74\pm0.005}$$

$$(N = 4, R = 0.9999)$$

$$[\mathrm{Mor}_{1,4}[\mathrm{Tf_2N}]: \tau_r = (2.62 \pm 0.05)\left(\frac{\eta}{T}\right)^{0.72\pm0.03}$$

$$(N = 5, R = 0.9969)$$

$$[\mathrm{Mor}_{1,6}][\mathrm{Tf_2N}]: \tau_r = (2.40 \pm 0.46)\left(\frac{\eta}{T}\right)^{0.52\pm0.03}$$

$$(N = 5, R = 0.9899)$$

$$[\mathrm{Mor}_{1,8}][\mathrm{Tf_2N}]: \tau_r = (1.89 \pm 0.030)\left(\frac{\eta}{T}\right)^{0.67\pm0.02}$$

$$(N = 5, R = 0.9972)$$

The low p values in hexyl and octyl chains containing ionic liquids also indicate that anthracene, like PRODAN, resides in the nonpolar domain formed by these long alkyl groups.

The excitation wavelength dependent measurements on AP and PRODAN also confirm the microheterogeneous nature of these RTILs. It can be seen from Table 1 that the rotational relaxation time in $[\mathrm{Mor}_{1,8}][\mathrm{Tf_2N}]$ is higher by 15% for AP and 40% for PRODAN for long wavelength excitation (439 nm)

dx.doi.org/10.1021/jp400914y | J. Phys. Chem. B 2013, 117, 5156−5164

near room temperature (25 °C). Figure 1 shows that the excitation wavelength dependence of the rotational time constants of AP in $[Mor_{1,8}][Tf_2N]$ is clearly observable near the room temperature, whereas in the case of PRODAN, it is observable even at higher temperatures. These results can be understood as follows. A longer wavelength (439 nm) excitation leads to preferential excitation of more (better) solvated molecules from the more polar region of the medium. These highly solvated molecules clearly experience more friction, thus exhibiting a longer rotational time compared to those located in the nonpolar domain that are preferentially excited at shorter wavelength (375 nm) excitation. A more prominent excitation wavelength dependence of PRODAN, which is observable over a longer temperature range, is indicative of a wider distribution of this molecule in different regions of the RTILs (compared to the other system) and persistence of the domain structure even at higher temperature.

A comparison of the present findings with those on rotational diffusion in imidazolium ionic liquids comprising alkyl chains of different lengths is quite pertinent here. While in one work a similar coupling constant and linear dependence of the rotational time τ_r values on η/T with increase in alkyl chain length of the imidazolium ion indicate that the chain length hardly influences the physical properties of these RTILs, or the changed properties hardly affect the solute rotation,[49] in another study, a change in physicochemical properties of these liquids with alkyl chain length of the cation was evident from the variation of the coupling constant values.[30,50] In our work, we could observe a steady change of the coupling constants and a high degree of nonlinearity of the τ_r values on η/T with increase in the alkyl chain length of the N-alkyl-N-methylmorpholinium cation, which not only indicate the changed physicochemical properties of these RTILs with variation of the alkyl group, but also establish the heterogeneous nature of these liquids that is more clearly evident in higher alkyl chain containing liquids.

4. CONCLUSION

Rotational dynamics of dipolar and nonpolar solutes in a series of N-alkyl-N-methylmorpholinium ionic liquids reveals their location in distinct environments of these media, depending on the nature of the solute. The stick to superstick behavior of AP, which is attributed to its H-bonding interaction with the constituent ions of the ionic liquids, reflects the most polar environment of the media. The slip to sub slip behavior of the nonpolar solute, anthracene, depicts the most nonpolar region of the ionic liquids formed largely by the alkyl group of the cation. On the other hand, the dipolar solute, PRODAN, which exhibits rotational time constant in between the slip and stick behavior, seems to be distributed in both regions. Excitation wavelength dependence of the rotational times of the dipolar probes also supports the heterogeneous environment of these RTILs. Overall, the present results provide further insight into the microheterogeneous structure of these ionic liquids, formed by the segregation of the alkyl chains on one hand and the charged components on the other. The study also points out how important the selection of the solute is for extracting information on the physicochemical properties of the complex media such as the ionic liquids.

■ ASSOCIATED CONTENT

Supporting Information

Plot of τ_r versus η/T for AP (Figure S1) and PRODAN (Figure S2) in different ionic liquids for the excitation wavelength of 439 nm along with the fitting parameters of dependence of τ_r on (η/T) according to $\tau_r = A(\eta/T)^p$ in each ionic liquid. Coupling constants for all sets of data are given in Table S1. This material is available free of charge via Internet at http://pubs.acs.org.

■ AUTHOR INFORMATION

Corresponding Author

*E-mail: assc@uohyd.ernet.in.

Notes

The authors declare no competing financial interest.

■ ACKNOWLEDGMENTS

This work has been supported by the J.C. Bose Fellowship (to A.S.) of the Department of Science and Technology, Government of India. D.C.K., J. P. K., and N.M. thank Council of Scientific and Industrial Research for Fellowship.

■ REFERENCES

(1) Hallett, J. P.; Welton, T. Room-Temperature Ionic Liquids: Solvents for Synthesis and Catalysis. 2. *Chem. Rev.* **2011**, *111*, 3508−3576.
(2) Dupont, J. From Molten Salts to Ionic Liquids: A "Nano" Journey. *Acc. Chem. Res.* **2011**, *44*, 1223−1231.
(3) Plechkova, N. V.; Seddon, K. R. Applications of Ionic Liquids in the Chemical Industry. *Chem. Soc. Rev.* **2008**, *37*, 123−150.
(4) Ionic Liquids (Special issue on ionic liquids). *Acc. Chem. Res.* **2007**, *40*, 1077−1236.
(5) The Physical Chemistry of Ionic Liquids (Special issue on ionic liquids). *J. Phys. Chem. B* **2007**, *111*, 4639−5029.
(6) The Physical Chemistry of Ionic Liquids (Special issue on ionic liquids). *Phys. Chem. Chem. Phys.* **2010**, *12*, 1629−2032.
(7) Hough, W. L.; Rogers, R. D. Ionic Liquids Then and Now: From Solvents to Materials to Active Pharmaceutical Ingredients. *Bull. Chem. Soc. Jpn.* **2007**, *80*, 2262−2269.
(8) Hough, W. L.; Smiglak, M.; Rodrıguez, H.; Swatloski, R. P.; Spear, S. K.; Daly, D. T.; Pernak, J.; Grisel, J. E.; Carliss, R. D.; Soutullo, M. D.; James H. Davis, J.; Rogers, R. D. The Third Evolution of Ionic Liquids: Active Pharmaceutical Ingredients. *New J. Chem.* **2007**, *31*, 1429−1436.
(9) Samanta, A. Solvation Dynamics in Ionic Liquids: What We Have Learned from the Dynamic Fluorescence Stokes Shift Studies. *J. Phys. Chem. Lett.* **2010**, *1*, 1557−1562.
(10) Kobrak, M. N. The Chemical Environment of Ionic Liquids: Links Between Liquid Structure, Dynamics and Solvation, In *Advances in Chemical Physics*, Rice, S. A., Ed.; John Wiley & Sons, Inc., 2008; Vol. *139*; pp 83−135.
(11) Huang, M. M.; Weingärtner, H. Protic Ionic Liquids with Unusually High Dielectric Permittivities. *ChemPhysChem* **2008**, *9*, 2172−2173.
(12) Castner, E. W., Jr.; Wishart, J. F. Spotlight on Ionic Liquids. *J. Chem. Phys.* **2010**, *132*, 120901(1−8).
(13) Samanta, A. Dynamic Stokes Shift and Excitation Wavelength Dependent Fluorescence of Dipolar Molecules in Room Temperature Ionic Liquids. *J. Phys. Chem. B* **2006**, *110*, 13704−13716.
(14) Daschakraborty, S.; Biswas, R. Ultrafast Solvation Response in Room Temperature Ionic Liquids: Possible Origin and Importance of the Collective and the Nearest Neighbour Solvent Modes. *J. Chem. Phys.* **2012**, *137*, 114501(1−11).
(15) Mandal, P. K.; Saha, S.; Karmakar, R.; Samanta, A. Solvation dynamics in room temperature ionic liquids: dynamic Stokes shift

studies of Fluorescence of Dipolar Molecules. *Curr. Sci.* **2006**, *90*, 301−310.
(16) Kim, K. S.; Choi, S.; Demberelnyamba, D.; Lee, H.; Oh, J.; Lee, B. B.; Mun, S. J. Ionic Liquids Based on N-alkyl-N-methylmorpholinium Salts as Potential Electrolytes. *Chem. Commun.* **2004**, 828−829.
(17) Lava, K.; Binnemans, K.; Cardinaels, T. Piperidinium, Piperazinium and Morpholinium Ionic Liquid Crystals. *J. Phys. Chem. B* **2009**, *113*, 9506−9511.
(18) Brigouleix, C.; Anouti, M.; Jacquemin, J.; Caillon-Caravanier, M.; Galiano, H.; Lemordant, D. Physicochemical Characterization of Morpholinium Cation Based Protic Ionic Liquids Used As Electrolytes. *J. Phys. Chem. B* **2010**, *114*, 1757−1766.
(19) Yu, W.; Peng, H.; Zhang, H.; Zhou, X. Synthesis and Mesophase Behaviour of Morpholinium Ionic Liquid Crystals. *Chin. J. Chem.* **2009**, *27*, 1471−1475.
(20) Khara, D. C.; Samanta, A. Fluorescence Response of Coumarin-153 in N-alkyl-N-methylmorpholinium Ionic Liquids: Are these Media More Structured Than the Imidazolium Ionic Liquids? *J. Phys. Chem. B* **2012**, *116*, 13430−13438.
(21) Russina, O.; Triolo, A.; Gontrani, L.; Caminiti, R. Mesoscopic Structural Heterogeneities in Room-Temperature Ionic Liquids. *J. Phys. Chem. Lett.* **2012**, *3*, 27−33.
(22) Patra, S.; Samanta, A. Microheterogeneity of Some Imidazolium Ionic Liquids As Revealed by Fluorescence Correlation Spectroscopy and Lifetime Studies. *J. Phys. Chem. B* **2012**, *116*, 12275−12283.
(23) Kashyap, H. K.; Hettige, J. J.; Annapureddy, H. V. R.; Margulis, C. J. SAXS Anti-Peaks Reveal the Length-Scales of Dual Positive−Negative and Polar−Apolar Ordering in Room-Temperature Ionic Liquids. *Chem. Commun.* **2012**, *48*, 5103−5105.
(24) Aoun, B.; Goldbach, A.; González, M. A.; Kohara, S.; Price, D. L.; Saboungi, M.-L. Nanoscale Heterogeneity in Alkyl-methylimidazolium Bromide Ionic Liquids. *J. Chem. Phys.* **2011**, *134*, 104509(1−7).
(25) Yamaguchi, T.; Miyake, S.; Koda, S. Shear Relaxation of Imidazolium-Based Room-Temperature Ionic Liquids. *J. Phys. Chem. B* **2010**, *114*, 8126−8133.
(26) Urahata, S. M.; Ribeiro, M. C. C. Unraveling Dynamical Heterogeneity in the Ionic Liquid 1-butyl-3-methylimidazolium Chloride. *J. Phys. Chem. Lett.* **2010**, *1*, 1738−1742.
(27) Shimomura, T.; Fujii, K.; Takamuku, T. Effects of the Alkyl-chain Length on the Mixing State of Imidazolium-based Ionic Liquid−methanol Solutions. *Phys. Chem. Chem. Phys.* **2010**, *12*, 12316−12324.
(28) Russina, O.; Gontrani, L.; Fazio, B.; Lombardo, D.; Triolo, A.; Caminiti, R. Selected Chemical−physical Properties and Structural Heterogeneities in 1-ethyl-3-methylimidazolium Alkyl-sulfate room Temperature Ionic Liquids. *Chem. Phys. Lett.* **2010**, *493*, 259−262.
(29) Hardacre, C.; Holbrey, J. D.; Mullan, C. L.; Youngs, T. G. A.; Bowron, D. T. Small Angle Neutron Scattering from 1-alkyl-3-methylimidazolium Hexafluorophosphate Ionic Liquids [$C_n$mim][PF_6], n=4, 6, and 8. *J. Chem. Phys.* **2010**, *133*, 074510(1−7).
(30) Fruchey, K.; Fayer, M. D. Dynamics in Organic Ionic Liquids in Distinct Regions Using Charged and Uncharged Orientational Relaxation Probes. *J. Phys. Chem. B* **2010**, *114*, 2840−2845.
(31) Bodo, E.; Gontrani, L.; Caminiti, R.; Plechkova, N. V.; Seddon, K. R.; Triolo, A. Structural Properties of 1-alkyl-3-methylimidazolium Bis{(trifluoromethyl)sulfonyl}amide Ionic Liquids: X-ray Diffraction Data and Molecular Dynamics Simulations. *J. Phys. Chem. B* **2010**, *114*, 16398−16407.
(32) Annapureddy, H. V. R.; Kashyap, H. K.; Biase, P. M. D.; Margulis, C. J. What is the Origin of the Prepeak in the X-ray Scattering of Imidazolium-Based Room-Temperature Ionic Liquids? *J. Phys. Chem. B* **2010**, *114*, 16838−16846.
(33) Xiao, D.; L., G. H., Jr.; Li, S.; Bartsch, R. A.; Quitevis, E. L.; Russina, O.; Triolo, A. Effect of Cation Symmetry and Alkyl Chain Length on the Structure and Intermolecular Dynamics of 1,3-dialkylimidazolium Bis(trifluoromethanesulfonyl)amide Ionic Liquids. *J. Phys. Chem. B* **2009**, *113*, 6426−6433.
(34) Habasaki, J.; Ngai, K. L. Heterogeneous Dynamics of Ionic Liquids from Molecular Dynamics Simulations. *J. Chem. Phys.* **2008**, *129*, 194501(1−15).
(35) Wang, Y.; Jiang, W.; Yan, T.; Voth, G. Understanding Ionic Liquids through Atomistic and Coarse-Grained Molecular Dynamics Simulations. A. *Acc. Chem. Res.* **2007**, *40*, 1193−1199.
(36) Triolo, A.; Russina, O.; Bleif, H. J.; Bleif, H. J.; Cola, E. D. Nanoscale Segregation in Room Temperature Ionic Liquids. *J. Phys. Chem. B* **2007**, *111*, 4641−4644.
(37) Rebelo, L. P. N.; Lopes, J. N. C.; Esperanca, J. M. S. S.; Guedes, H. J. R.; Lachwa, J.; Najdanovic-Visak, V.; Visak, Z. P. Accounting for the Unique, Doubly Dual Nature of Ionic Liquids from a Molecular Thermodynamic and Modeling Standpoint. *Acc. Chem. Res.* **2007**, *40*, 1114−1121.
(38) Iwata, K.; Okajima, H.; Saha, S.; Hamaguchi, H. O. Local Structure Formation in Alkyl-imidazolium-Based Ionic Liquids as Revealed by Linear and Nonlinear Raman Spectroscopy. *Acc. Chem. Res.* **2007**, *40*, 1174−1181.
(39) Xiao, D.; Rajian, J. R.; Li, S.; Bartsch, R. A.; Quitevis, E. L. Additivity in the Optical Kerr Effect Spectra of Binary Ionic Liquid Mixtures: Implications for Nanostructural Organization. *J. Phys. Chem. B* **2006**, *110*, 16174−16178.
(40) Wang, Y.; Voth, G. A. Tail Aggregation and Domain Diffusion in Ionic Liquids. *J. Phys. Chem. B* **2006**, *110*, 18601−18608.
(41) Shigeto, S.; Hamaguchi, H. O. Evidence for Mesoscopic Local Structures in Ionic Liquids: CARS Signal Spatial Distribution of $C_n$mim[PF_6] (n = 4,6,8). *Chem. Phys. Lett.* **2006**, *427*, 329−332.
(42) Lopes, J. C.; Gomes, M. F. C.; Padua, A. A. H. Nonpolar, Polar, and Associating Solutes in Ionic Liquids. *J. Phys. Chem. B* **2006**, *110*, 16816−16818.
(43) Lopes, J. A. C.; Padua, A. A. H. Nanostructural Organization in Ionic Liquids. *J. Phys. Chem. B* **2006**, *110*, 3330−3335.
(44) Hu, Z.; Margulis, C. Heterogeneity in a Room-Temperature Ionic Liquid: Persistent Local Environments and the Red-Edge Effect. *J. Proc. Natl. Acad. Sci. U. S. A.* **2006**, *103*, 831−836.
(45) Wang, Y.; Voth, G. A. Unique Spatial Heterogeneity in Ionic Liquids. *J. Am. Chem. Soc.* **2005**, *127*, 12192−12193.
(46) Daschakraborty, S.; Biswas, R. Does Polar Interaction Influence Medium Viscosity? A Computer Simulation Investigation Using Model Liquids. *J. Chem. Sci.* **2012**, *124*, 763−771.
(47) Karve, L.; Dutt, G. B. Rotational Diffusion of Neutral and Charged Solutes in 1-butyl-3-methylimidazolium-Based Ionic Liquids: Influence of the Nature of the Anion on Solute Rotation. *J. Phys. Chem. B* **2012**, *116*, 1824−1830.
(48) Karve, L.; Dutt, G. B. Role of Specific Interactions on the Rotational Diffusion of Organic Solutes in a Protic Ionic Liquid−Propylammonium Nitrate. *J. Phys. Chem. B* **2012**, *116*, 9107−9113.
(49) Gangamallaiah, V.; Dutt, G. B. Rotational Diffusion of Nonpolar and Ionic Solutes in 1-alkyl-3-methylimidazolium Bis-(trifluoromethylsulfonyl)imides: Is Solute Rotation Always Influenced by the Length of the Alkyl Chain on the Imidazolium Cation? *J. Phys. Chem. B* **2012**, *116*, 12819−12825.
(50) Das, S. K.; Sarkar, M. Rotational Dynamics of Coumarin-153 and 4-Aminophthalimide in 1-ethyl-3-methylimidazolium Alkylsulfate Ionic Liquids: Effect of Alkyl Chain Length on the Rotational Dynamics. *J. Phys. Chem. B* **2012**, *116*, 194−202.
(51) Karve, L.; Dutt, G. B. Rotational Diffusion of Neutral and Charged Solutes in Ionic Liquids: Is Solute Reorientation Influenced by the Nature of the Cation? *J. Phys. Chem. B* **2011**, *115*, 725−729.
(52) Khara, D. C.; Samanta, A. Rotational Dynamics of Positively and Negatively Charged Solutes in Ionic Liquid and Viscous Molecular Solvent Studied by Time-resolved Fluorescence Anisotropy Measurements. *Phys. Chem. Chem. Phys.* **2010**, *12*, 7671−7677.
(53) Dutt, G. B. Rotational Diffusion of Nondipolar Solutes in Ionic Liquids: Influence of the Nature of Anion on Solute Rotation. *Indian J. Chem.* **2010**, *49A*, 705−713.
(54) Dutt, G. B. Influence of Specific Interactions on the Rotational Dynamics of Charged and Neutral Solutes in Ionic Liquids Containing Tris(pentafluoroethyl)trifluorophosphate (FAP) Anion. *J. Phys. Chem. B* **2010**, *114*, 8971−8977.
(55) Mali, K. S.; Dutt, G. B.; Mukherjee, T. Rotational Diffusion of a Nonpolar and a Dipolar Solute in 1-butyl-3-methylimidazolium

Hexafluorophosphate and Glycerol: Interplay of Size Effects and Specific Interactions. *J. Chem. Phys.* **2008**, *128*, 054504(1−9).
(56) Jin, H.; Baker, G. A.; Arzhantsev, S.; Dong, J.; Maroncelli, M. Solvation and Rotational Dynamics of Coumarin 153 in Ionic Liquids: Comparisons to Conventional Solvents. *J. Phys. Chem. B* **2007**, *111*, 7291−7302.
(57) Ito, N.; Arzhantsev, S.; Maroncelli, M. The Probe Dependence of Solvation Dynamics and Rotation in the Ionic Liquid 1-butyl-3-methyl-Imidazolium Hexafluorophosphate. *Chem. Phys. Lett.* **2004**, *396*, 83−91.
(58) Ito, N.; Arzhantsev, S.; Heitz, M.; Maroncelli, M. Solvation Dynamics and Rotation of Coumarin 153 in Alkylphosphonium Ionic Liquids. *J. Phys. Chem. B* **2004**, *108*, 5771−5777.
(59) Ingram, J. A.; Moog, R. S.; Ito, N.; Biswas, R.; Maroncelli, M. Solute Rotation and Solvation Dynamics in a Room-Temperature Ionic Liquid. *J. Phys. Chem. B* **2003**, *107*, 5926−5932.
(60) Das, S. K.; Sahu, P. K.; Sarkar, M. Diffusion−Viscosity Decoupling in Solute Rotation and Solvent Relaxation of Coumarin153 in Ionic Liquids Containing Fluoroalkylphosphate (FAP) Anion: A Thermophysical and Photophysical Study. *J. Phys. Chem. B* **2013**, *113*, 636−647.
(61) Zvaigzne, A. I.; Wolfe, J.; William E. Acree, J. Solubility of Anthracene in Solvent Mixtures Binary Alkane + 2-methyl-1 -propanol. *J. Chem. Eng. Data* **1994**, *39*, 541−543.
(62) Geddes, C. D.; Lakowicz, J. R., Eds.; *Reviews in Fluorescence*; Springer: New York, 2005; pp 199−222.
(63) Horng, M. L.; Gardecki, J. A.; Maroncelli, M. Rotational Dynamics of Coumarin 153: Time-Dependent Friction, Dielectric Friction, and Other Nonhydrodynamic Effects. *J. Phys. Chem. A* **1997**, *101*, 1030−1047.
(64) Anderton, R. M.; Kauffman, J. F. Temperature-Dependent Rotational Relaxation of Diphenylbutadiene in n-Alcohols: A Test of the Quasihydrodynamic Free Space Model. *J. Phys. Chem.* **1994**, *98*, 12117−12124.
(65) Roy, M.; Doraiswamy, S. Rotational Dynamics of Nonpolar Solutes in Different Solvents: Comparative Evaluation of the Hydrodynamic and Quasihydrodynamic models. *J. Chem. Phys.* **1993**, *98*, 3213−3223.
(66) Ben-Amotz, D.; Drake, J. M. The Solute Size Effect in Rotational Diffusion Experiments: A Test of Microscopic Friction Theories. *J. Chem. Phys.* **1988**, *89*, 1019−1029.
(67) Spernol, A.; Wirtz, K. Molekulare Theorie der Mikroreibeng. *Z. Nuturforsch. A* **1953**, *8*, 532−538.
(68) Edward, J. T. Molecular Volumes and the Stokes-Einstein Equation. *J. Chem. Educ.* **1970**, *47*, 261−270.
(69) Paul, A.; Samanta, A. Solute Rotation and Solvation Dynamics in an Alcohol-Functionalized Room Temperature Ionic Liquid. *J. Phys. Chem. B* **2007**, *111*, 4724−4731.
(70) Guchhait, B.; Gazi, H. A. R.; Kashyap, H. K.; Biswas, R. Fluorescence Spectroscopic Studies of (Acetamide + Sodium/Potassium Thiocyanates) Molten Mixtures: Composition and Temperature Dependence. *J. Phys. Chem. B* **2010**, *114*, 5066−5081.
(71) Faetti, M.; Giordano, M.; Leporini, D.; Pardi, L. Scaling Analysis and Distribution of the Rotational Correlation Times of a Tracer in Rubbery and Glassy Poly(vinyl acetate): An Electron Spin Resonance Investigation. *Macromolecules* **1999**, *32*, 1876−1882.
(72) Andreozzi, L.; Faetti, M.; Giordano, M.; Leporini, D. Scaling of the Rotational Relaxation of Tracers in o-Terphenyl: A Linear and Nonlinear ESR Study. *J. Phys. Chem. B* **1999**, *103*, 4097−4103.
(73) Andreozzi, L.; Schino, A. D.; Giordano, M.; Leporini, D. Evidence of a fractional Debye-Stokes-Einstein law in supercooled o-terphenyl. *Europhys. Lett.* **1997**, *38*, 669−674.
(74) The trend of a steady decrease of C_{rot} value with the van der Waals volume of RTILs is, however, not so clear at higher temperature in the case of anthracene.